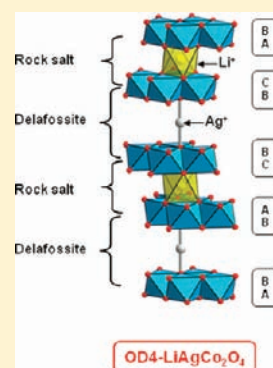


# (Li/Ag)CoO<sub>2</sub>: A New Intergrowth Cobalt Oxide Composed of Rock Salt and Delafossite Layers

R. Berthelot,<sup>†,‡</sup> M. Pollet,<sup>\*,†</sup> J.-P. Doumerc,<sup>†</sup> and C. Delmas<sup>†,§</sup><sup>†</sup>CNRS, Université de Bordeaux, ICMCB, 87 avenue du Dr. A. Schweitzer, 33608 F-Pessac, France<sup>‡</sup>CEA-Grenoble, DRT-LITEN, 17 rue des Martyrs, 38054 Grenoble, France<sup>§</sup>CNRS, ENSCBP, ICMCB, 87 avenue du Dr. A. Schweitzer, 33608 F-Pessac, France

**ABSTRACT:** A new ordered (Li/Ag)CoO<sub>2</sub> layered compound with an unusual oxygen packing combining rock salt and delafossite layers is obtained during the (Li<sup>+</sup>, Na<sup>+</sup>)/Ag<sup>+</sup> ionic exchange from the OP4-(Li/Na)CoO<sub>2</sub> precursor. This compound is actually an intermediate step to the final D4-AgCoO<sub>2</sub> delafossite and can be isolated thanks to the kinetics difference between the Li<sup>+</sup>/Ag<sup>+</sup> and Na<sup>+</sup>/Ag<sup>+</sup> exchange processes. It crystallizes in the *P6<sub>3</sub>/mmc* space group with cell parameters  $a_{\text{hex.}} = 2.848(3)$  Å and  $c_{\text{hex.}} = 21.607(7)$  Å. The details of the structure as well as its thermal stability and transport properties are presented and discussed.



## 1. INTRODUCTION

The very details of the structure of layered ACoO<sub>2</sub> oxides like stacking sequences or local symmetries are assumed to have a key role on their remarkable properties, such as the electrochemical behavior of the high-temperature polytype of LiCoO<sub>2</sub>, which is the most commercialized positive electrode material for lithium batteries,<sup>1</sup> or the fascinating properties reported for P2-Na<sub>x</sub>CoO<sub>2</sub> phases depending on their sodium content<sup>2</sup> (promising thermoelectric properties for high-sodium compositions,<sup>3–5</sup> superconductivity for hydrated phases at  $x \sim 0.3$ ,<sup>6,7</sup> or metal to insulator transition for the half-filled Na<sub>1/2</sub>CoO<sub>2</sub><sup>8</sup>).

The structure of all these materials can be described from a packing of CoO<sub>2</sub> slabs, formed by edge-shared CoO<sub>6</sub> octahedra, between which A<sup>+</sup> monovalent cations are intercalated in the interslab space. Depending on the nature of the A element, its content ( $x$ ), and the synthesis conditions, various intercalation sites are available: octahedral in O3-, O2-, and O4-LiCoO<sub>2</sub><sup>9–12</sup> and O3-NaCoO<sub>2</sub>,<sup>13,14</sup> trigonal prismatic in P2- and P3-Na<sub>x</sub>CoO<sub>2</sub> or -K<sub>x</sub>CoO<sub>2</sub>,<sup>13–16</sup> tetrahedral in deintercalated bilayered Li<sub>x</sub>CoO<sub>2</sub>,<sup>17</sup> or linear dumbbell in the case of the delafossite structure, where A is typically a d<sup>10</sup> or d<sup>9</sup> monovalent cation like, for instance, a noble metal.<sup>18–24</sup> In order to standardize the description of the layered ACoO<sub>2</sub> oxides, we follow the nomenclature proposed by Delmas et al.<sup>25</sup> using as a prefix of the chemical formulas the combination of a letter that stands for the A cation site symmetry (O for octahedron, P for trigonal prism, and D for dumbbell coordination) and a figure indicating the number of CoO<sub>2</sub> layers necessary to describe the structure.

Recently, we used the ordered OP4-Li<sub>~0.42</sub>Na<sub>~0.37</sub>CoO<sub>2</sub> phase, which was originally reported for its promising thermoelectric properties,<sup>26–28</sup> as a precursor for ionic exchanges, and we first reported on the two new layered polytypes obtained, O4-LiCoO<sub>2</sub><sup>12</sup>

and D4-AgCoO<sub>2</sub>,<sup>29</sup> which regularly alternates O2/O3- and D2/D3-type blocks, respectively. The structure of such polytypes with new oxygen stacking is directly related to the original structure of the OP4-(Li/Na)CoO<sub>2</sub> precursor that alternates two different AO<sub>2</sub> blocks: a P2-type sodium block and an O3-type lithium one (Figure 1a).<sup>30</sup> While the site symmetry could change through the ionic exchange, the layer organization remains the same as in the OP4 precursor, leaving unchanged the number of CoO<sub>2</sub> slabs necessary to describe the final hexagonal cell (i.e., four slabs). The exchange process may induce or not a slab gliding in the  $a, b$  plane but never a slab rotation, as such an operation would require a Co–O bond breaking that only occurs at high temperature and was never observed in the vicinity of room temperature.

During the OP4 → O4 transformation, which was also studied by Komaba et al.,<sup>31</sup> only Na<sup>+</sup> ions are exchanged and the OP4 precursor directly gives the O4 stacking without any intermediate step. In the case of the OP4 → D4 transformation, however, both Na<sup>+</sup> and Li<sup>+</sup> ions are exchanged for silver ones. During this process, we noticed the presence of traces of an intermediate phase OD4-(Li/Ag)CoO<sub>2</sub> combining rock salt and delafossite blocks (Figure 1b). This report details the structure of this new OD4-(Li/Ag)CoO<sub>2</sub> intergrowth layered cobalt oxide, explains its formation by the kinetics difference between Na<sup>+</sup>/Ag<sup>+</sup> and Li<sup>+</sup>/Ag<sup>+</sup> exchanges, and presents preliminary measurements of physical properties.

## 2. EXPERIMENTAL SECTION

**2.1. Synthesis of the Precursors.** Several authors have reported on the synthesis of the OP4-(Li/Na)CoO<sub>2</sub> precursor with some nuances

Received: March 15, 2011

Published: June 16, 2011

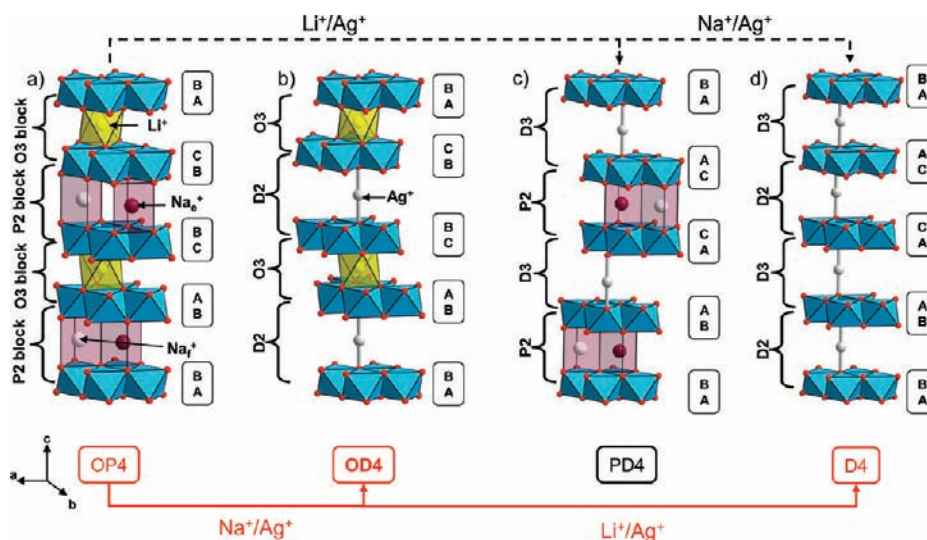


**Figure 1.** Perspective representation of (a) the ordered OP4-(Li/Na)CoO<sub>2</sub> precursor and the three stacking that may theoretically be obtained from (Li<sup>+</sup>+Na<sup>+</sup>)/Ag<sup>+</sup> ionic exchanges; (b) the OD4-(Li/Ag)CoO<sub>2</sub> studied in this article; (c) the PD4-(Na/Ag)CoO<sub>2</sub>, which is not evidenced due to difference in the Li<sup>+</sup>/Ag<sup>+</sup> and Na<sup>+</sup>/Ag<sup>+</sup> exchange kinetics; and (d) the delafossite D4-AgCoO<sub>2</sub> obtained after the complete exchange of the alkali ions.<sup>29</sup> In these structures, lithium and sodium ions occupy respectively octahedral (in yellow) or trigonal prismatic sites (in light purple), while silver ions are intercalated in a dumbbell configuration. Sodium ions accommodate two kinds of trigonal prismatic sites depending on whether they share face (Na<sub>f</sub>, in white) or edges (Na<sub>e</sub>, in purple) with surrounding CoO<sub>6</sub> octahedra. For convenience, only one intercalated site is sketched in each interslab space. The oxygen stacking sequence is written next to each structure.

in the synthesis protocol and in the chemical composition, but most of them agree on the difficulty to obtain a pure phase.<sup>26–28,30</sup> We recently deeply reinvestigated the synthesis path and proposed a more pertinent protocol.<sup>32</sup> In brief, the precursors O3-LiCoO<sub>2</sub> and P2-Na<sub>~0.7</sub>CoO<sub>2</sub> were first prepared from solid-state reactions using dry alkali carbonates and cobalt oxide Co<sub>3</sub>O<sub>4</sub> that were intimately ground. A stoichiometric ratio was used for the preparation of O3-LiCoO<sub>2</sub>, while an excess of 5 wt % of sodium carbonate was added for the preparation of P2-Na<sub>~0.7</sub>CoO<sub>2</sub> in order to balance to sodium oxide volatility at high temperature. These mixtures were heated at 850 and 900 °C for 24 h under oxygen flow with heating and cooling rates set at +2 and –5 °C min<sup>–1</sup>, respectively. Following our previous work,<sup>32</sup> these two precursors were then intimately mixed together in the nominal composition Li<sub>0.42</sub>Na<sub>~0.41</sub>CoO<sub>2</sub> in an argon-filled glovebox. The mixture was put into a gold tube that was quickly sealed and then heated for at least 1 day at 920 °C in a preheated furnace. The tube was finally quenched in a water bath. Such thermal treatment avoids the decomposition of the OP4-(Li/Na)CoO<sub>2</sub> phase.<sup>32</sup> All the compounds being moisture sensitive, they were stored in a dry atmosphere. Rietveld refinement on XRD pattern (not shown) confirmed the synthesis of pure OP4-Li<sub>~0.42</sub>Na<sub>~0.37</sub>CoO<sub>2</sub> precursors with cell parameters in good agreement with the literature.<sup>30</sup> The slight loss of sodium may be explained by (i) the difficult control of the initial Na content in the P2-Na<sub>~0.7</sub>CoO<sub>2</sub> precursor or (ii) a weak Na departure (as oxide) in the free void of the sealed gold tube (indeed some white deposits were sometimes noticed in the gold tube after synthesis). However, the calculated chemical formula totally agrees with the already published compositions.<sup>26,30</sup>

**2.2. Ionic Exchanges.** Following previous works dealing with silver delafossites synthesis,<sup>21–23,33,34</sup> ionic exchanges in molten salts were performed by mixing the OP4-(Li/Na)CoO<sub>2</sub> precursor with silver nitrate and potassium nitrate. In the case of the pure D4-AgCoO<sub>2</sub> synthesis, a preliminary ball-milling of the powder precursor as well as a large silver nitrate excess (5 times compare to alkali nominal content), a high temperature, and a long dwell time (15 h at ~300 °C) were necessary to complete the exchange.<sup>29</sup> In this work, the goal was to only exchange the Na<sup>+</sup> ions with no departure of the Li<sup>+</sup> ions from the O3-type blocks.

It was therefore necessary to increase the selectivity of the exchange, and several kinetic and thermodynamic parameters were adjusted to maximize the Na<sup>+</sup>/Ag<sup>+</sup> exchange rate while the Li<sup>+</sup>/Ag<sup>+</sup> exchange one was minimized. Following our previous study on the D4-AgCoO<sub>2</sub> compound, for which we noticed that the grain size reduction was an important parameter since without ball-milling the obtaining of the pure D4 synthesis systematically failed (small amounts of OD4-(Li/Ag)CoO<sub>2</sub> remained, as seen in XRD patterns), we fixed the grain size to that of the as-synthesized OP4 powder, i.e., as large as possible. The other parameters were tuned as follows: the temperature of the melt was varied from 300 °C down to 130 °C using a mixture of AgNO<sub>3</sub>/KNO<sub>3</sub> at the eutectic molar ratio 3/2<sup>35</sup>); for lower temperature trials down to room temperature, the OP4 precursor was immersed in a AgNO<sub>3</sub> aqueous solution; this approach assumes a two-step reaction:



We also tuned the silver and lithium concentrations in the molten salts in order to create supplementary driving forces to hinder the second step (i.e., the D4 formation): the nominal Na<sup>+</sup>/Ag<sup>+</sup> ratio was tuned to 1, while lithium nitrate was added up from 2 to 10 times excess (as compared to the lithium amount in the OP4 precursor). Concerning the heat treatment, the dwell time at high temperature was varied from 15 to 2 h.

**2.3. Characterizations.** XRD measurements were performed using a PANalytical X'Pert Pro powder diffractometer in the Bragg–Brentano geometry using either copper or cobalt K $\alpha$  radiation. Data were collected using an X'Celerator detector in the 10°–80° window in the 2 $\theta$  range. High-temperature experiments were performed in an Anton Paar HTK 1200N oven chamber under dry oxygen flow (+1 °C min<sup>–1</sup> mean rate until 700 °C and –10 °C min<sup>–1</sup> to cool until room temperature).

The chemical composition was determined by inductively coupled plasma absorption electron spectroscopy (ICP-AES) on a Varian 720-ES. For alkali lamellar oxides, samples were dissolved in HCl solution heated to ~70 °C. For samples containing silver, HNO<sub>3</sub> solution was sometimes

additionally used as complement when the dissolution was difficult to complete.

The average grain size of the powder samples was determined with a Malvern Mastersizer 2000 particle size analyzer by immersing the powder in ethanol bath, with a preliminary ultrasonic step to break up the biggest aggregates.

Thermogravimetric analysis (TGA) were performed with an STD Q600 apparatus under Ar flow (initial dwell of 2 h at 100 °C, heating rate +5 °C min<sup>-1</sup>, final dwell of 30 min at 700 °C, cooling rate -5 °C min<sup>-1</sup>).

Transport properties were measured on nonsintered, compacted pellets. Electrical dc resistivity was performed with the four-probe method in the 4–300 K range, while thermoelectric power measurements were collected with homemade equipment previously described.<sup>36</sup>

### 3. ORDERED STACKING SIMULATION

Two different layered structures can be sketched assuming different selective exchanges for the lithium or sodium cations: either an OD4-(Li/Ag)CoO<sub>2</sub> phase that alternates O3-type lithium layers and D2-type silver layers (Figure 1b, resulting from the selective exchange of only sodium ions) or a PD4-(Na/Ag)CoO<sub>2</sub> phase that combines P2-type sodium layers and D3-type silver layers (Figure 1c, resulting from the selective exchange of only lithium ions). Actually, there are several arguments in favor of a preferential exchange of Na<sup>+</sup> ions compared to Li<sup>+</sup> ones: (i) the ions diffusion through face-sharing trigonal prisms is easier than through octahedra, which requires the ions to pass through an intermediate tetrahedral site; (ii) the interslab space AO<sub>2</sub> (A = Li, Na) increase that is necessary to accommodate the Ag<sup>+</sup> ions is smaller for the Na<sup>+</sup>/Ag<sup>+</sup> exchange (~+16%) than for the Li<sup>+</sup>/Ag<sup>+</sup> one (~+56%) (these values are calculated by comparing the interslab thicknesses in OP4-Li<sub>0.42</sub>Na<sub>0.37</sub>CoO<sub>2</sub><sup>32</sup> and in AgCoO<sub>2</sub><sup>21,37</sup>); and (iii) a slab gliding is required during the Li<sup>+</sup>/Ag<sup>+</sup> exchange, while no oxygen packing change is needed for the Na<sup>+</sup>/Ag<sup>+</sup> exchange. As the Na<sup>+</sup> ions should be removed more easily than the Li<sup>+</sup> ions, the theoretical PD4 phase should not appear during the OP4 → D4 process.

In our previous works, we simulated the O4-LiCoO<sub>2</sub> and the D4-AgCoO<sub>2</sub> polytypes using as input parameters some previous experimental crystallographic data for O2-LiCoO<sub>2</sub>,<sup>10,38,11</sup> O3-LiCoO<sub>2</sub>,<sup>9</sup> and AgCoO<sub>2</sub>,<sup>18,21–23,37</sup> like the cation–oxygen distances and the thicknesses of CoO<sub>2</sub> slabs and AO<sub>2</sub> interslab spaces, to build up the new blocks of the O4 and D4 polytypes, respectively.<sup>12,29</sup> This approach was also extended to the description of the ordered OPP9-(Li/Na/Na)CoO<sub>2</sub> packing that alternates within the lamellar CoO<sub>2</sub> stacking two P2 sodium layers for one O3 lithium layer.<sup>32</sup> We applied this method in the present study to sketch the OD4-(Li/Ag)CoO<sub>2</sub> and the PD4-(Na/Ag)CoO<sub>2</sub> stacking.

The required input parameters needed are the thicknesses of LiO<sub>2</sub>, NaO<sub>2</sub>, and AgO<sub>2</sub> interslabs.<sup>9,15,37</sup> These two stackings are then built up by superimposing O3 and D2 blocks or P2 and D3 blocks for respectively the OD4 and the PD4 compound. The thicknesses of the CoO<sub>2</sub> slabs are averaged between the two parent phases, as well as *a*<sub>hex</sub> parameters (Table 1); the *z* positions of the cations are adjusted at the center of the slabs and interslabs.

A crystallographic symmetry operator determination led to the *P*6<sub>3</sub>/*mmc* space group in both cases, with lattice parameters *a*<sub>hex</sub> = 2.845 Å and *c*<sub>hex</sub> = 21.613 Å for OD4 and *a*<sub>hex</sub> = 2.853 Å and *c*<sub>hex</sub> = 23.126 Å for PD4. For the OD4-(Li/Ag)CoO<sub>2</sub> phase, the atomic positions are given in Table 2 and the corresponding simulated XRD pattern is plotted in Figure 2d.

**Table 1. Structural Data Used To Simulate the OD4 and PD4 sStacking**

	OD4-(Li/Ag)CoO <sub>2</sub>	PD4-(Na/Ag)CoO <sub>2</sub>
space group		<i>P</i> 6 <sub>3</sub> / <i>mmc</i>
<i>a</i> <sub>hex</sub> (Å)	2.845 <sup>a</sup>	2.853 <sup>b</sup>
<i>c</i> <sub>hex</sub> (Å)	21.613	23.126
CoO <sub>2</sub> slab thickness (Å)	1.985 <sup>a</sup>	1.944 <sup>b</sup>
AO <sub>2</sub> interslab thickness (Å)	2.633 for A = Li	3.471 for A = Na 4.204 for A = Ag

<sup>a</sup> Obtained from P2-Na<sub>0.7</sub>CoO<sub>2</sub><sup>15</sup> and D3-AgCoO<sub>2</sub><sup>37</sup> average. <sup>b</sup> Obtained from O3-LiCoO<sub>2</sub><sup>9</sup> and D2-AgCoO<sub>2</sub><sup>37</sup> average.

**Table 2. Atomic Position of the OD4-(Li/Ag)CoO<sub>2</sub> from the Stacking Simulation in the *P*6<sub>3</sub>/*mmc* Space Group<sup>a</sup>**

atom	site	<i>x</i>	<i>y</i>	<i>z</i>	occ
Ag	2b	0	0	1/4	1
Li	2a	0	0	1/2	0.84
Co	4f	2/3	1/3	0.393	1
O	4e	0	0	0.347	1
O	4f	1/3	2/3	0.439	1

<sup>a</sup> The lithium occupancy factor is set to 0.84 assuming a theoretical composition OD4-Li<sub>0.42</sub>Ag<sub>0.5</sub>CoO<sub>2</sub>.

## 4. RESULTS AND DISCUSSIONS

**4.1. Ionic Exchanges.** Figure 2a presents the XRD pattern obtained after a first ionic exchange with the OP4-(Li/Na)CoO<sub>2</sub> precursor (experimental conditions: (Li<sup>+</sup> + Na<sup>+</sup>)/Ag<sup>+</sup> ratio close to 1, thermal treatment of 15 h at ~300 °C, final washing step). The profile matching refinement evidences two phases that both crystallize in the *P*6<sub>3</sub>/*mmc* space group: the D4-AgCoO<sub>2</sub> delafossite according to our previous work<sup>29</sup> and a new phase for which the diffraction pattern nicely compares with the simulated pattern of an OD4-(Li/Ag)CoO<sub>2</sub> (Figure 2d). Moreover, there is not any trace of the OP4-(Li/Na)CoO<sub>2</sub> precursor. A possible PD4-(Na/Ag)CoO<sub>2</sub> phase formation is totally discarded here. The ICP-AES analysis realized after washing of the product reveals that the sodium content is insignificant, clearly confirming that the Na<sup>+</sup>/Ag<sup>+</sup> exchange is completely achieved.

In order to roughly quantify the phase proportions, Rietveld refinement was performed using the simulated structural data of the D4<sup>29</sup> and the OD4 phases by only varying the cell parameters as well as the profile parameters (the structural parameters were fixed). The D4 delafossite appeared to be the majority phase (~5/6). In addition, the refinement gives OD4 lattice parameters [*a*<sub>hex</sub> = 2.848(3) Å and *c*<sub>hex</sub> = 21.607(7) Å], in rather good agreement with our simulation work (Table 1).

The presence of this intermediate phase is related to the different mechanism implied for the lithium and sodium exchanges. For these reasons, the lithium exchange requires high activation energy and lower grain size as well as higher temperature, dwell time and silver concentration are at the same time necessary to make the exchange complete.

Decreasing the temperature to ~130 °C while the dwell time is shortened to only 2 h and the (Li<sup>+</sup> + Na<sup>+</sup>)/Ag ratio is lowered to ~2 (i.e., Na/Ag ~1) significantly improves the results, as the OD4-(Li/Ag)CoO<sub>2</sub> phase becomes the majority: the intensity of the (004) diffraction peak of the D4-AgCoO<sub>2</sub> delafossite clearly

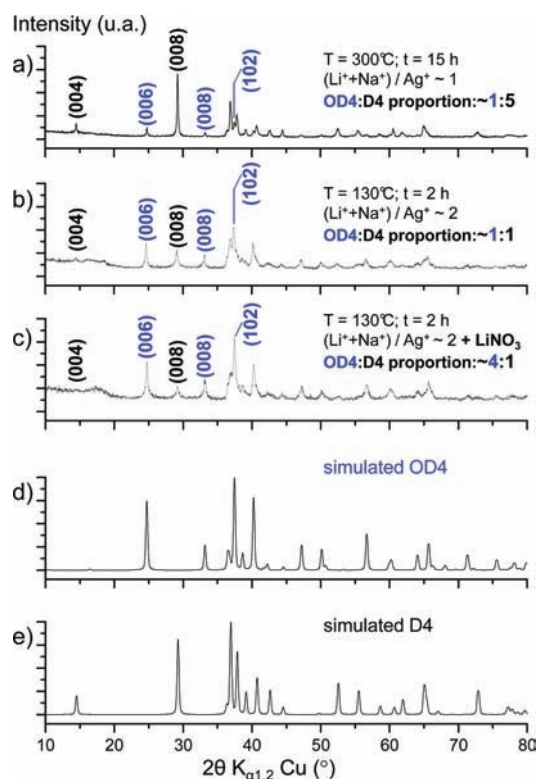


**Figure 2.** (a–c) Experimental XRD data obtained after different ionic exchanges from the OP4-(Li/Na)CoO<sub>2</sub> raw material. For comparison, the calculated XRD pattern obtained from the simulation of (d) OD4-(Li/Ag)CoO<sub>2</sub> (from Table 2) and (e) D4-AgCoO<sub>2</sub> (from ref 29) are shown.

decreases while the (006) and (008) diffraction peak intensities of the OD4-(Li/Ag)CoO<sub>2</sub> phase increase (Figure 2b). Quantitatively, a Rietveld refinement gives approximately half of the OD4 phase in the final product.

The addition of lithium nitrate in the salt (in 2 times molar excess as compared to the initial lithium amount in the precursor powder) significantly hinders the lithium exchange and finally stabilizes the OD4 phase up to about 80% (Figure 2c); however, tuning further this parameter no longer improves the results, and we could not get a complete elimination of the D4-AgCoO<sub>2</sub> phase. In order to further decrease the reaction temperature several exchange reactions in water solution were tested from boiling point to room temperature, using equivalent [Ag<sup>+</sup>] and [Li<sup>+</sup>] concentrations as above. The OD4 formation is evidenced in all cases, but OP4-(Li/Na)CoO<sub>2</sub> still remains present in majority while the D4-AgCoO<sub>2</sub> delafossite diffraction peaks are clearly appearing in all XRD patterns (not shown), even for stirring times as short as 2 h, at room temperature. To conclude, we managed to increase the proportion of the obtained OD4 phase by tuning some reaction parameters; however, we did not succeed to completely avoid the Li<sup>+</sup>/Ag<sup>+</sup> ionic exchange.

The broadening of the diffraction lines of both OD4 and D4 phases might be attributed to stacking defects that occur during the ionic exchange process. For example, one can reasonably assume the presence of sporadic D4 blocks in the overall OD4 structure.

Note also that for all the ionic exchanges that use a high [Li<sup>+</sup>] concentration in the solution, a competition between silver and lithium to replace sodium can be expected. In the latter case, the O4-LiCoO<sub>2</sub> polytype could be formed.<sup>12,31</sup> The XRD patterns, however, never showed any presence of this compound, whatever

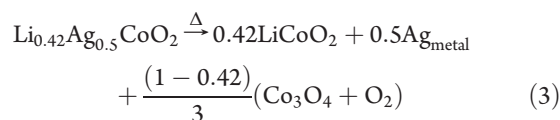
the magnitude of the other parameters; this confirms that the slab gliding (necessary in the Na<sup>+</sup>/Li<sup>+</sup> exchange) is more energy consuming than the increase of the interslab thickness and that it is the limiting factor for the exchange.

ICP-AES analyses were not appropriate to determine the precise composition of the OD4 phase, mainly because powders were difficult to dissolve. However, one can notice that (i) the OP4 precursor is characterized by lithium vacancies<sup>30,26–28</sup> and (ii) previous reports on silver delafossites obtained by ionic exchanges from P2-Na<sub>0.7</sub>CoO<sub>2</sub> conclude the stoichiometric composition Ag<sub>1</sub>CoO<sub>2</sub>.<sup>18,24</sup> According to these results and assuming that (i) the lithium layers remain unchanged during the ionic exchange process, (ii) silver ions cannot enter into lithium interslab space as the oxygen stacking is not suitable for accommodating the dumb-bell coordination, and (iii) silver ions completely fill the sodium interslab space, the chemical composition of the OD4 phase should be close to Li<sub>0.42</sub>Ag<sub>0.5</sub>CoO<sub>2</sub>.

In conclusion of this experimental section, the OD4-(Li/Ag)CoO<sub>2</sub> formation is clearly evidenced to be an intermediate step in the global OP4 → D4 ionic exchange. All our attempts to isolate this phase pure were unsuccessful and it appeared impossible from this method to replace all the sodium ions before starting the exchange of lithium ions.

**4.2. Thermal Stability.** Ionic exchange reactions often lead to metastable phases, such as the O4- and the O2-LiCoO<sub>2</sub> polytypes, which turn into the thermodynamically stable O3 polytype when they are heated.<sup>11,12,38</sup> Silver delafossites are also sensitive to temperature as they decompose into metallic silver and cobalt oxide Co<sub>3</sub>O<sub>4</sub> below 600 °C.<sup>29</sup> According to these remarks, we first performed an in situ XRD experiment on an initial mixture of the OD4 and the D4 phases obtained with the best above-mentioned conditions (corresponding XRD in Figure 2c). Figure 3 shows the XRD pattern evolution vs temperature in the 6.5°–60° 2θ range. Up to 400 °C, the temperature increase causes a narrowing of diffraction peaks [highlighted in the inset of Figure 3 focusing on the (006) peak of the OD4 phase], which can be explained by an enhancement of the crystallinity of each phase.

In the same temperature range, however, characteristic diffraction peaks of O3-LiCoO<sub>2</sub>, Co<sub>3</sub>O<sub>4</sub>, and metallic silver already begin to grow. At ~550 °C, all the (00*l*) diffraction peaks of the OD4 phase have vanished. This experiment clearly demonstrates the instability of the OD4 phase, which decomposes according to the eq 3 (with the assumption of the initial chemical composition Li<sub>0.42</sub>Ag<sub>0.5</sub>CoO<sub>2</sub>).



The D4 delafossite also decomposes just after the OD4 by giving additional Co<sub>3</sub>O<sub>4</sub> and metallic silver, in agreement with our previous results.<sup>29</sup>

**4.3. Morphology Characterization.** The grain morphology of a sample containing the OD4 and the D4 phases (corresponding XRD in Figure 2c) are shown in Figure 4. The micrograph analysis cannot distinguish the different phases, as the grain size and morphology appear very homogeneous. The large grain size (>10 μm) results from the absence of a preliminary milling step before the ionic exchange. The lamellar shape is clearly visible, especially with micrographs focused on the edges of the particles. Despite some sporadic particles that keep the hexagonal shape (highlighted by white dot lines), most of the particles are

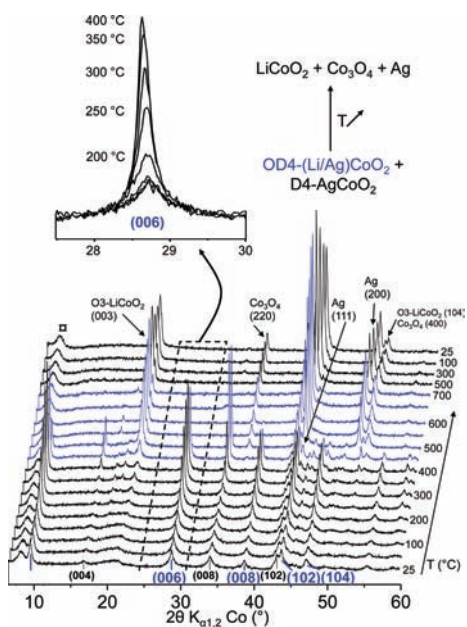


**Figure 3.** Temperature influence on the XRD powder pattern of an initial mixture of OD4-(Li/Ag)CoO<sub>2</sub> and D4-AgCoO<sub>2</sub> phases in a 4:1 ratio (corresponding to sample c in Figure 2). The O3-LiCoO<sub>2</sub>, Co<sub>3</sub>O<sub>4</sub>, and metallic silver diffraction peaks begin to grow in the 350–450 °C temperature range, reflecting the decomposition of the OD4-(Li/Ag)CoO<sub>2</sub> phase. The delafossite D4-AgCoO<sub>2</sub> decomposition occurs from 500 °C. The inset focuses on the evolution of the (006) diffraction peak of the OD4 phase and highlights the crystallinity enhancement at the beginning of the heating sequence. The symbol (x) marks the peak of the polymer window of the airtight in situ cell.

characterized by a more rounded contour. A similar morphology characterizes the OP4 precursor (Figure 4), but it is more stressed after the ionic exchange that alters the shape of the grains.

**4.4. Electrical Properties.** Depending on the A element, lamellar oxides ACoO<sub>2</sub> exhibit different kinds of transport properties: an insulator behavior is obtained in ACoO<sub>2</sub> delafossites with A = Cu, Ag, while a metallic one is obtained for A = Pd, Pt; O3-LiCoO<sub>2</sub> is insulating, but Li<sub>x<1</sub>CoO<sub>2</sub> materials become more and more conductive and even metallic as Li<sup>+</sup> is further deintercalated;<sup>39</sup> the OP4-(Li/Na)CoO<sub>2</sub> precursor exhibits interesting thermoelectric properties with a large Seebeck coefficient coexisting with a relatively good electrical conductivity.<sup>26,27</sup>

The study of the electrical properties of OD4-(Li/Ag)CoO<sub>2</sub> is complicated because of (i) its poor thermal stability that prevent any sintering, (ii) the presence of the secondary D4 phase that could not be fully eliminated, and (iii) the anisotropy of the structure that could lead to a strong anisotropy of the electrical properties as in the case of delafossite oxides.<sup>20</sup> The physical measurements were finally performed on nonsintered compacted pellets (bulk density close to 70%) containing a mixture of roughly 4:1 OD4:D4 (i.e., with the sample characterized by the XRD pattern of Figure 2c). Figure 5 displays the temperature dependence of the electrical resistivity and of the thermopower in the temperature range 5–300 K and compares them with the behavior of pure D4-AgCoO<sub>2</sub>.<sup>29</sup> Regarding the above three limitations, the transport measurements are not expected to give access to intrinsic properties but only to reflect some trends in the global behavior of the new phase. The OD4/D4 sample displays a global insulator behavior with a resistivity decreasing with temperature.

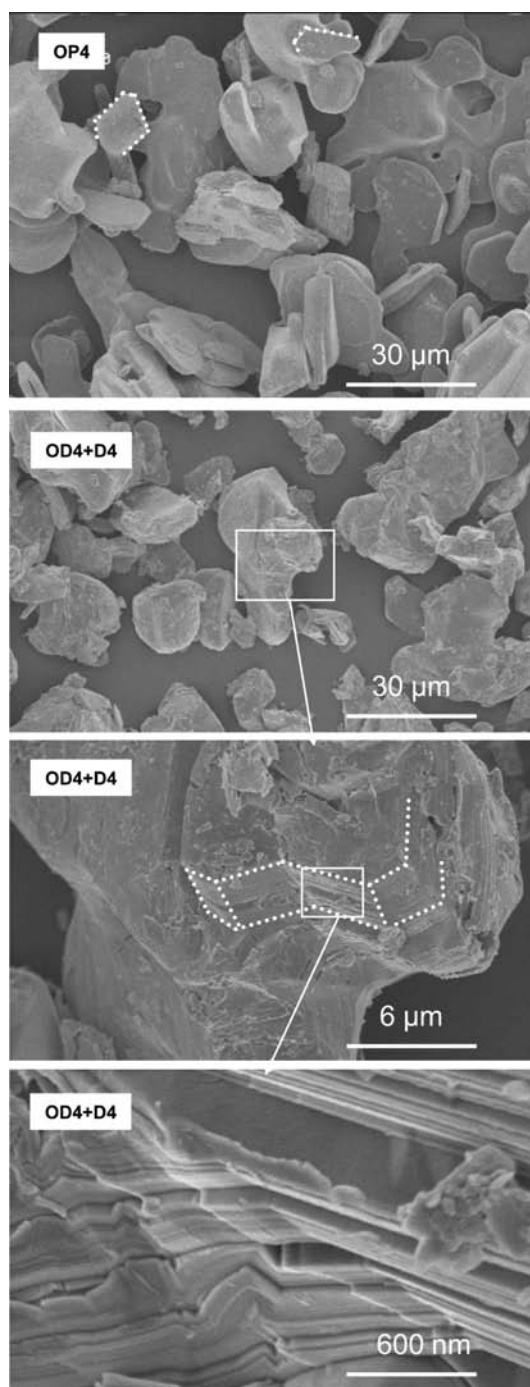


**Figure 4.** SEM micrographs of powder sample of the 4:1 mixture of the OD4 and the D4 phases at three different magnifications and of the OP4-(Li/Na)CoO<sub>2</sub> for comparison. The white dotted lines highlight the particle hexagonal shape.

The Seebeck coefficient is positive and its temperature dependence follows a monotonous and roughly linear increase up to room temperature. Such a behavior shows that charge carriers are holes diffusing through a hopping mechanism. In comparison with pure D4-AgCoO<sub>2</sub>, the OD4/D4 mixture sample exhibits a lower resistivity and a lower thermopower, which is in agreement with a larger charge-carrier concentration, as expected from the nominal compositions. Determining whether holes are moving within silver layers, like in most delafossite oxides,<sup>20</sup> or in cobalt

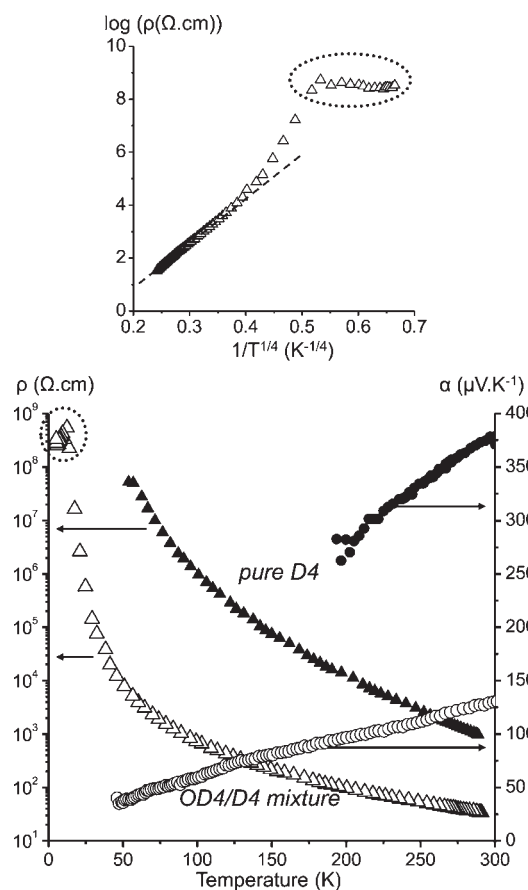


**Figure 5.** Evolution vs temperature of the resistivity (triangles) and of the Seebeck coefficient (circles) measured on nonsintered, compacted pellets of the 4:1 mixture of OD4 and D4 phases (white marks) and of a pure D4-AgCoO<sub>2</sub> (black marks, from ref 29). (Inset) Evidence, with the dashed line, of the variable range hopping conduction behavior in the ~50–300 K temperature range.

layers is out of the scope of the present paper in view of the experimental limitations above-mentioned. In the second hypothesis, the thermopower value at room temperature would be far below the asymptotic value expected from the Heikes formula ( $\sim 260 \mu\text{V K}^{-1}$ ) for the given sample composition and assuming the usual electronic configuration for cobalt(III) and -(IV) located in the relevant site symmetry.<sup>40</sup>

As shown in the inset of Figure 5 and as already observed for pure D4-AgCoO<sub>2</sub> delafossite,<sup>29</sup> the resistivity data obey a Mott's law of the form  $\rho = A \exp[(T_0/T)^{1/4}]$ .<sup>41,42</sup> However, below ca. 50 K, Mott's law is no longer obeyed, and, below 15 K, the electrical resistivity no longer decreases as the temperature is further decreased. Such a behavior is rarely observed in experimental studies of semiconducting oxides, but it was predicted as a possible transport mechanism at low temperature ( $T < \Theta_D/2$ , where  $\Theta_D$  is the Debye temperature) when the zero point energy  $1/2h\nu$  associated with quantum fluctuations can take the place of thermal vibrations.<sup>43</sup>

## 5. CONCLUSION

A new lamellar phase alternating rock salt and delafossite type layers is evidenced as an intermediate step during the global OP4-(Li/Na)CoO<sub>2</sub>  $\rightarrow$  D4-AgCoO<sub>2</sub> ionic exchange. The easier

exchange of Na<sup>+</sup> ions (as compared to Li<sup>+</sup> ions) for Ag<sup>+</sup> explains the existence of this OD4-(Li/Ag)CoO<sub>2</sub> phase, which is the second example of a mixed ordered (A/A')CoO<sub>2</sub> packing after the OP4-(Li/Na)CoO<sub>2</sub> and the first case of an intergrowth of rock salt and delafossite layers. The space group is  $P6_3/mmc$  and the cell parameters are  $a_{\text{hex.}} = 2.848(3) \text{ \AA}$  and  $c_{\text{hex.}} = 21.607(7) \text{ \AA}$ , in perfect agreement with simulation studies. Tuning different thermodynamic and kinetic parameters enables one to impede the D4 delafossite formation, but within our experimental setup we could not avoid any Li<sup>+</sup>/Ag<sup>+</sup> ionic exchange; the best result is a mixture of ~80% of the OD4 phase and ~20% of the D4 phase.

As other ionic exchange products, the OD4-(Li/Ag)CoO<sub>2</sub> phase is not stable and tends to decompose above 400–450 °C, giving O3-LiCoO<sub>2</sub>, Co<sub>3</sub>O<sub>4</sub>, and metallic silver. Electrical measurements performed on a nonsintered, compacted pellet of a 4:1 mixture of OD4 and D4 reveal a semiconductor behavior.

## AUTHOR INFORMATION

### Corresponding Author

\*E-mail: pollet@icmcb-bordeaux.cnrs.fr.

## ACKNOWLEDGMENT

The authors want to thank J. Villot, S. Fourcade, C. Denage, L. Etienne, E. Lebraud, and S. Pechev for technical assistance and ANR OCTE for financial support. CEA is also thanked for a scholarship to R.B.

## REFERENCES

- Mizushima, K.; Jones, P.; Wiseman, P.; Goodenough, J. *Mater. Res. Bull.* **1980**, *15* (6), 783.
- Berthelot, R.; Carlier, D.; Delmas, C. *Nat. Mater.* **2011**, *10* (1), 74.
- Terasaki, I.; Sasago, Y.; Uchinokura, K. *Phys. Rev. B Condens. Matter Mater. Phys.* **1997**, *56* (20), R12685.
- Lee, M.; Viciu, L.; Li, L.; Wang, Y.; Foo, M.; Watauchi, S.; Pascal, R., Jr.; Cava, R.; Ong, N. *Nat. Mater.* **2006**, *5* (7), 537.
- Lee, M.; Viciu, L.; Li, L.; Wang, Y.; Foo, M.; Watauchi, S.; Pascal, R., Jr.; Cava, R.; Ong, N. *Phys. B Condens. Matter* **2008**, *403* (5–9), 1564.
- Takada, K.; Sakurai, H.; Takayama-Muromachi, E.; Izumi, F.; Dilanian, R.; Sasaki, T. *Nature* **2003**, *422* (6927), 53.
- Schaak, R.; Klimczuk, T.; Foo, M.; Cava, R. *Nature* **2003**, *424* (6948), 527.
- Huang, Q.; Foo, M.; Lynn, J.; Zandbergen, H.; Lawes, G.; Wang, Y.; Toby, B.; Ramirez, A.; Ong, N.; Cava, R. *J. Phys.: Condens. Matter* **2004**, *16* (32), 5803.
- Levasseur, S.; Ménétrier, M.; Suard, E.; Delmas, C. *Solid State Ionics* **2000**, *128* (1–4), 11.
- Delmas, C.; Braconnier, J.-J.; Hagenmuller, P. *Mater. Res. Bull.* **1982**, *17* (1), 117.
- Carlier, D.; Saadoune, I.; Croguennec, L.; Ménétrier, M.; Suard, E.; Delmas, C. *Solid State Ionics* **2001**, *144* (3–4), 263.
- Berthelot, R.; Carlier, D.; Pollet, M.; Doumerc, J.-P.; Delmas, C. *Electrochem. Solid-State Lett.* **2009**, *12* (11), A207.
- Fouassier, C.; Matejka, G.; Reau, J.-M.; Hagenmuller, P. *J. Solid State Chem.* **1973**, *6* (4), 532.
- Viciu, L.; Bos, J.; Zandbergen, H.; Huang, Q.; Foo, M.; Ishiwata, S.; Ramirez, A.; Lee, M.; Ong, N.; Cava, R. *Phys. Rev. B Condens. Matter Mater. Phys.* **2006**, *73* (17), 174104.
- Huang, Q.; Foo, M.; Pascal, R., Jr.; Lynn, J.; Toby, B.; He, T.; Zandbergen, H.; Cava, R. *Phys. Rev. B Condens. Matter Mater. Phys.* **2004**, *70* (18), 184110.
- Blangero, M.; Decourt, R.; Carlier, D.; Ceder, G.; Pollet, M.; Doumerc, J.-P.; Darriet, J.; Delmas, C. *Inorg. Chem.* **2005**, *44* (25), 9299.

- (17) Carlier, D.; Croguennec, L.; Ceder, G.; Ménétrier, M.; Shao-Horn, Y.; Delmas, C. *Inorg. Chem.* **2004**, *43* (3), 914.
- (18) Shannon, R. D.; Rogers, D. B.; Prewitt, C. T. *Inorg. Chem.* **1971**, *10* (4), 713.
- (19) Prewitt, C.; Shannon, R.; Rogers, D. *Inorg. Chem.* **1971**, *10* (4), 719.
- (20) Rogers, D.; Shannon, R.; Prewitt, C.; Gillson, J. *Inorg. Chem.* **1971**, *10* (4), 723.
- (21) Shin, Y.; Doumerc, J.-P.; Dordor, P.; Pouchard, M.; Hagenmuller, P. *J. Solid State Chem.* **1993**, *107* (1), 194.
- (22) Shin, Y.; Doumerc, J.-P.; Pouchard, M.; Hagenmuller, P. *Mater. Res. Bull.* **1993**, *28* (2), 159.
- (23) Shin, Y.-J.; Kwak, J.-H.; Yoon, S. *Bull. Korean Chem. Soc.* **1997**, *18* (7), 775.
- (24) Muguerra, H.; Colin, C.; Anne, M.; Julien, M.-H.; Strobel, P. *J. Solid State Chem.* **2008**, *181* (11), 2883.
- (25) Delmas, C.; Fouassier, C.; Hagenmuller, P. *Phys. B+C (Amsterdam, Neth.)* **1980**, *99* (1–4), 81.
- (26) Ren, Z.; Shen, J.; Jiang, S.; Chen, X.; Feng, C.; Xu, Z.; Cao, G. *J. Phys.: Condens. Matter* **2006**, *18* (29), L379.
- (27) Chen, X.; Xu, X.-F.; Hu, R.-X.; Ren, Z.; Xu, Z.-A.; Cao, G.-H. *Acta Phys. Sin.* **2007**, *56*, 1627.
- (28) Bos, J.; Hertz, J.; Morosan, E.; Cava, R. *J. Solid State Chem.* **2007**, *180* (11), 3211.
- (29) Berthelot, R.; Pollet, M.; Doumerc, J.-P.; Delmas, C. *Inorg. Chem.* **2011**, *50* (10), 4529.
- (30) Balsys, R.; Lindsay Davis, R. *Solid State Ionics* **1994**, *69* (1), 69.
- (31) Komaba, S.; Yabuuchi, N.; Kawamoto, Y. *Chem. Lett.* **2009**, *38* (10), 954.
- (32) Berthelot, R.; Pollet, M.; Carlier, D.; Delmas, C. *Inorg. Chem.* **2011**, *50* (6), 2420.
- (33) Doumerc, J.-P.; Ammar, A.; Wichainchai, A.; Pouchard, M.; Hagenmuller, P. *J. Phys. Chem. Solids* **1987**, *48* (1), 37.
- (34) Ammar, A. *Contribution à l'étude des oxydes de type delafossite: Corrélations entre propriétés cristalochimiques et électroniques*. Ph.D. thesis, University of Marrakech, 1988.
- (35) Ussow, A. Z. *Anorg. Allg. Chem.* **1904**, *38* (1), 419.
- (36) Dordor, P.; Marquestaut, E.; Villeneuve, G. *Rev. Phys. Appl.* **1980**, *15*, 1607.
- (37) Seshadri, R.; Felser, C.; Thieme, K.; Tremel, W. *Chem. Mater.* **1998**, *10* (8), 2189.
- (38) Paulsen, J.; Mueller-Neuhaus, J.; Dahn, J. *J. Electrochem. Soc.* **2000**, *147* (2), 508.
- (39) Ménétrier, M.; Saadoune, I.; Levasseur, S.; Delmas, C. *J. Mater. Chem.* **1999**, *9* (5), 1135.
- (40) Pollet, M.; Doumerc, J.-P.; Guilmeau, E.; Grebille, D.; Fagnard, J.-F.; Cloots, R. *J. Appl. Phys.* **2007**, *101* (8), 083708.
- (41) Mott, N. F.; Davis, E. A. *Electronic Process in Non-Crystalline Materials*; Clarendon Press: Oxford, 1979.
- (42) Cox, P. *Transition Metal Oxides: An Introduction to Their Electronic Structure and Properties*; Clarendon Press: Oxford, 1995.
- (43) Mott, N. F. *Metal–Insulator Transitions*; Taylor & Francis: London, 1990.